VISCOELASTIC FLOWS OVER A SLOT: A STABILIZED FINITE ELEMENT INVESTIGATION

Renato da Rosa Martins, renato@mecanica.ufrgs.br
Sérgio Frey, frey@mecanica.ufrgs.br
Laboratory of Theoretical and Computational Mechanics (LAMAC), Mechanical Engineering Department, Universidade Federal do Rio Grande do Sul, Rua Sarmento Leite, 425, 90050-170, Porto Alegre, RS, Brazil

Maria Laura Martins-Costa, laura@mec.uff.br
Laboratory of Theoretical and Applied Mechanics (LMTA), Mechanical Engineering Graduate Program (PGMEC), Universidade Federal Fluminense, Rua Passo da Pátria, 156, 24210-240 Niterói, RJ, Brazil

Abstract. *Most industrial synthetic fluid behavior cannot be described by the Newtonian model – unable to characterize phenomena such as shear-thinning, non-null stress differences or memory effects. This article is concerned with stabilized finite element simulations for a viscoelastic fluid flowing through a slot. A multi-field Galerkin least-squares (GLS) method in terms of extra-stress, velocity and pressure is used to approximate the flows – which are modeled by considering the usual mass and momentum balance equations for incompressible fluids linked to the Oldroyd-B viscoelastic differential model. The GLS formulation circumvents the need to compatibilize pressure-velocity (the so-called Babuška-Brezzi condition) and stress-velocity subspaces, allowing employing equal-order finite elements. The influence of viscolelastic and inertia effects on the flow patterns is considered by ranging Deborah number from 0 to 0.26 and varying Reynolds number from 0 to 20. The numerical results are able to characterize accurately viscoelastic flows subjected to inertia.*

Keywords*: Oldroyd-B fluid, inertia effects, multifield Galerkin-least squares formulation, finite elements in fluids.*

1. INTRODUCTION

Most industrial synthetic fluids applications deal with fluids presenting a behavior that cannot be described by the linear (Newtonian) model, since the stress applied on the fluid is no longer directly proportional to the strain caused in the material, with the proportionality constant being known as the fluid viscosity. Non-Newtonian fluids may present complex phenomena such as shear-thinning, non-null stress differences or memory effects. The first one, responsible for the shear thinning of the viscosity, is usual in most non-Newtonian flows, being well described by the generalized Newtonian liquid (GNL) model (Bird et al., 1987). Despite its large use, the GNL model can predict neither memory effects nor the elastic non-null normal stress differences. In order to predict this behavior many viscoelastic differential models have been proposed in the last decades, among which the Maxwell-B and the Oldroyd-B models deserve special attention, due to their straight computational implementation and their good performance for low Deborah number flows.

This article is focused on the numerical simulation of an upper-convected Oldroyd fluid – known as Oldroyd-B fluid – flowing over a slot (Cochrane et al., 1981) – a very well known benchmark employed in the pressure correction of fluid flows. For the particular case of viscoelastic fluid flows, such a flow is used to evaluate normal stress effects – being usually called a pressure hole problem (Sugeng et al., 1988; Tanner, 2000). The Oldroyd-B model, which may be viewed as a polymer solution composed by an elastic polymer dissolved in a viscous Newtonian solvent, diminishes the difficulty of handling numerically with an elastic Maxwell fluid – with a convective-type evolution equation – by the addition of a Newtonian solvent (Behr et al., 2004).

Classical Galerkin approximation of incompressible flows shows some difficulties (Johnson, 1987), the first one is to match the finite element sub-spaces of velocity and pressure, satisfying the classic Babuška-Brezzi condition (Babuška, 1971; Brezzi, 1974). The second difficulty appears in multi-field formulations: the choice of the finite elements sub-spaces of stress and velocity. The third one would be the instability inherent to centered discretization schemes in addressing advective dominated problems, due to the asymmetry of the advective operator, that may cause an oscillatory behavior of Galerkin discretization, which can get worse due to the non-linearities present in the constitutive models for non-Newtonian fluids.

The GLS method uses a least-squares formulation to build the perturbation terms, increasing the stability of the original Galerkin formulation, without harming its consistency. This methodology has already been largely used to treat structural problems and fluid flows (Franca and Frey, 1992; Franca et al., 1994). The additional terms come from a minimization of the least-squares of the residues of the Galerkin formulation, adding an *upwind* effect in the flow streamlines direction (Brooks and Hughes, 1982; Franca et al., 1992) in addition to modifying the Galerkin classic formulation, requiring neither the satisfaction of the inf-sup condition (Hughes et al., 1986) nor the compatibility of velocity and extra stress subspaces. This feature is particularly relevant when a viscoelastic model is considered, since it

lessens the difficulty of handling with the extra-stress by considering it as a primal variable. Also, the traction term is present in the GLS formulation, allowing natural imposition of free-surface boundary conditions (Behr et al., 2004).

Finite elements multifield formulations have been largely employed for simulating flows of non-Newtonian fluids. Baaijens (1998), in a review article, discussed the developments of mixed finite elements in the approximation of viscoelastic flows, including stabilizing strategies. Behr et al. (2004) simulated an Oldroyd-B flow past a cylinder in a channel, varying the Weissenberg number and employing a GLS tree field formulation. Many researchers have simulated interesting geometries with viscoelastic flows employing finite volume methodologies. Alves et al. (2003) have simulated flows through a 4:1 sudden contraction of both Oldroyd-B and PTT fluids employing a fully implicit finite volume method, based on a time-marching pressure correction algorithm, presenting results for vortex size, vortex intensity and pressure drop. In a subsequent work, Alves et al. (2004), investigated the contraction ratio effect on PTT fluid flow though an abrupt contraction, combining a finite volume method with a high resolution scheme for the convective terms discretization, considering contraction ratios of 10, 20, 40 and 100.

In this work, the flow of an Oldroyd-B fluid in a slot is simulated by a multi-field GLS formulation, in which the computational domain is partitioned using a bilinear Lagrangian finite element mesh with 3200 elements rendering 19200 degrees of freedom. Such a combination (employing equal-order finite elements) violates the compatibility conditions of the classical Galerkin method involving the finite elements subspaces for stress-pressure-velocity. The numerical simulation was performed aiming at undertaking a sensitivity analysis, in order to evaluate the influence of the elastic and inertia effects on the flow pattern. These tasks are carried out investigating the Deborah (De) and Reynolds (Re) numbers, respectively, in relevant ranges i. e., from De=0 to De=0.26 and from Re=0 to Re=20; the former being limited by the discontinuity of the stress field introduced by the sharp corners of the geometry, and the latter by the usually high viscosity of the macromolecular fluids.

2. MECHANICAL MODEL

Mass and momentum conservation equations for steady-state incompressible isothermal flows are given by

$$\begin{aligned} &\operatorname{div}\mathbf{u} = 0 \\ &\rho\left(\nabla\mathbf{u}\right)\mathbf{u} = -\nabla p + \operatorname{div}\boldsymbol{\tau} + \mathbf{f} \end{aligned} \tag{1}$$

where the Cauchy stress tensor has been decomposed as $\boldsymbol{\sigma} = -\,p\,\mathbf{I} + \boldsymbol{\tau}$, p being the hydrodynamic pressure and $\boldsymbol{\tau}$ the extra stress tensor; $\mathbf{u}$ the fluid velocity vector and $\mathbf{f}=\rho\mathbf{g}$ the gravitational force per unit volume ($\mathbf{g}$ being the gravitational acceleration). In this work the extra stress tensor presents a viscoelastic behavior, according to the Oldroyd-B model; which may be viewed as an elastic Maxwell fluid – a polymer with extra-stress $\boldsymbol{\tau}_1$ – dissolved in a viscous Newtonian fluid with extra-stress $\boldsymbol{\tau}_2$, its constitutive evolutionary character being expressed as (Oldroyd, 1958; Behr et al, 2004)

$$\begin{aligned} &\boldsymbol{\sigma} = -p\mathbf{I} + \boldsymbol{\tau} \\ &\boldsymbol{\tau} = \boldsymbol{\tau}_1 + \boldsymbol{\tau}_2 \\ &\boldsymbol{\tau}_1 + \lambda\overset{\nabla}{\boldsymbol{\tau}}_1 = 2\eta_1\mathbf{D}\left(\mathbf{u}\right) \\ &\boldsymbol{\tau}_2 = 2\eta_2\mathbf{D}\left(\mathbf{u}\right) \\ &\eta_1 + \eta_2 = \eta \end{aligned} \tag{2}$$

where $\eta_1 = \eta_p$ is the viscosity of the elastic polymer, λ is its relaxation time, $\eta_2 = \eta_s$ is the viscosity of the viscous solvent, $\mathbf{D}(\mathbf{u})$ is the rate-of-strain tensor and the upper-convected derivative for steady-state regimen is expressed as

$$\overset{\nabla}{\boldsymbol{\tau}} = \left(\nabla\boldsymbol{\tau}\right)\mathbf{u} - \left(\nabla\mathbf{u}\right)\boldsymbol{\tau} - \boldsymbol{\tau}\left(\nabla\mathbf{u}\right)^{T} \tag{3}$$

Thus, combining the mass and momentum balance equations with the constitutive assumption given by Eq. (2) and incorporating the boundary conditions, the mechanical model concerned herein for a multi-field boundary value problem, defined by the triple extra shear stress, pressure and velocity fields, and the associated system of contact and body forces, may be stated as:

$$
\begin{aligned}
&\rho\left[\left(\nabla\mathbf{u}\right)\mathbf{u}\right]+\nabla p-\operatorname{div}\boldsymbol{\tau}-2\eta_s\mathbf{D}\left(\mathbf{u}\right)=\mathbf{f} && \text{in } \Omega\\
&\boldsymbol{\tau}-\lambda\left[\left(\nabla\boldsymbol{\tau}\right)\mathbf{u}-\left(\nabla\mathbf{u}\right)\boldsymbol{\tau}-\boldsymbol{\tau}\left(\nabla\mathbf{u}\right)^T\right]=2\eta_p\mathbf{D}\left(\mathbf{u}\right) && \text{in } \Omega\\
&\operatorname{div}\mathbf{u}=0 && \text{in } \boldsymbol{\Omega}\\
&\mathbf{u}=\mathbf{u}_g && \text{on } \Gamma_g\\
&\left[\boldsymbol{\tau}-p\mathbf{I}\right]\mathbf{n}=\mathbf{t}_h && \text{on } \Gamma_h
\end{aligned}
\tag{4}
$$

where $\mathbf{u}$, p, $\mathbf{f}$, $\boldsymbol{\tau}$, ρ, λ, η_p, η_s, and $\mathbf{D}(\mathbf{u})$ have been previously defined and Γ_g is the portion of the boundary Γ (of the region Ω) in which Dirichlet boundary condition is imposed, with $\mathbf{u}_g$ representing a prescribed velocity field, while Γ_h is the part of Γ where Neumann boundary condition is imposed, being $\mathbf{n}$ the unit outward normal and $\mathbf{t}_h$ the traction vector.

3. FINITE ELEMENT APPROXIMATION

Based on the usual definitions of the subspaces for shear stress ($\boldsymbol{\Sigma}^h$), velocity ($\mathbf{V}^h$) and pressure (P^h) (Behr *et al.*, 1993), it is possible to write a Galerkin least-squares (GLS) multi-field formulation by using the numerical strategy proposed by Behr *et al.* (1993) for fluids with constant viscosity and subsequently employed by Zinani and Frey (2008), considering a viscosity function dependent on the shear rate, which can be extended for viscoelastic flows. The GLS formulation for the problem defined by Eq. (4), is written as: *Find the triple* $(\boldsymbol{\tau}^h, p^h, \mathbf{u}^h) \in \Sigma^h \times P^h \times \mathbf{V}_g^h$ *such that*:

$$
B\left(\boldsymbol{\tau}^h, p^h, \mathbf{u}^h, \mathbf{S}^h, q^h, \mathbf{v}^h\right) = F\left(\mathbf{S}^h, q^h, \mathbf{v}^h\right) \qquad \forall\left(\mathbf{S}^h, q^h, \mathbf{v}^h\right) \in \boldsymbol{\Sigma}^h \times P^h \times \mathbf{V}_g^h \tag{5}
$$

where

$$
\begin{aligned}
&B\left(\boldsymbol{\tau}^h, p^h, \mathbf{u}^h; \mathbf{S}^h, q^h, \mathbf{v}^h\right) = \left(2\eta_p\right)^{-1}\int_\Omega \boldsymbol{\tau}^h\cdot\mathbf{S}^h d\Omega + 2\eta_s\int_\Omega \mathbf{D}\left(\mathbf{u}^h\right)\cdot\mathbf{D}\left(\mathbf{v}^h\right)d\Omega - \int_\Omega \mathbf{D}\left(\mathbf{u}^h\right)\cdot\mathbf{S}^h d\Omega\\
&+\left(2\eta_p\right)^{-1}\int_\Omega \lambda\left[\left(\nabla\boldsymbol{\tau}^h\right)\mathbf{u}^h - \left(\nabla\mathbf{u}^h\right)\boldsymbol{\tau}^h - \boldsymbol{\tau}^h\left(\nabla\mathbf{u}^h\right)^T\right]\cdot\mathbf{S}^h d\Omega + \delta\left(\mathrm{Re}_K\right)\int_\Omega \operatorname{div}\mathbf{u}^h\ \operatorname{div}\mathbf{v}^h d\Omega\\
&+\int_\Omega \rho\left(\nabla\mathbf{u}^h\right)\mathbf{u}^h\cdot\mathbf{v}^h d\Omega + \int_\Omega \boldsymbol{\tau}^h\cdot\mathbf{D}(\mathbf{v}^h)d\Omega - \int_\Omega p^h\cdot\operatorname{div}\mathbf{v}^h d\Omega + \int_\Omega \operatorname{div}\mathbf{u}^h\ q^h d\Omega + \varepsilon\int_\Omega p^h\ q^h d\Omega\\
&+\sum_{K\in\Omega^h}\int_{\Omega_k}\left(\rho\left(\nabla\mathbf{u}^h\right)\mathbf{u}^h + \nabla p^h - 2\eta_s\operatorname{div}\mathbf{D}\left(\mathbf{u}^h\right) - \operatorname{div}\boldsymbol{\tau}^h\right)\cdot\alpha\left(\mathrm{Re}_K\right)\left(\rho\left(\nabla\mathbf{v}^h\right)\mathbf{u}^h + \nabla q^h - 2\eta_s\operatorname{div}\mathbf{D}\left(\mathbf{v}^h\right) - \operatorname{div}\mathbf{S}^h\right)d\Omega\\
&+2\eta_p\beta\int_\Omega\left\{\left(2\eta_p\right)^{-1}\boldsymbol{\tau}^h + \left(2\eta_p\right)^{-1}\lambda\left[\left(\nabla\boldsymbol{\tau}^h\right)\mathbf{u}^h - \left(\nabla\mathbf{u}^h\right)\boldsymbol{\tau}^h - \boldsymbol{\tau}^h\left(\nabla\mathbf{u}^h\right)^T\right] - \mathbf{D}\left(\mathbf{u}^h\right)\right\}\cdot\\
&\quad\cdot\left\{\left(2\eta_p\right)^{-1}\mathbf{S}^h + \left(2\eta_p\right)^{-1}\lambda\left[\left(\nabla\mathbf{S}^h\right)\mathbf{u}^h - \left(\nabla\mathbf{u}^h\right)\mathbf{S}^h - \mathbf{S}^h\left(\nabla\mathbf{u}^h\right)^T\right] - \mathbf{D}\left(\mathbf{v}^h\right)\right\}d\Omega
\end{aligned}
\tag{6}
$$

and

$$
F\left(\mathbf{S}^h, q^h, \mathbf{v}^h\right) = \int_\Omega \mathbf{f}\cdot\mathbf{v}^h d\Omega + \int_{\Gamma_h}\mathbf{t}_h\cdot\mathbf{v}^h d\Gamma + \sum_{K\in\Omega^h}\int_\Omega \mathbf{f}\cdot\alpha\left(\mathrm{Re}_K\right)\left[\rho\left(\nabla\mathbf{v}^h\right)\mathbf{u}^h + \nabla q^h - 2\eta_s\operatorname{div}\mathbf{D}\left(\mathbf{u}^h\right) - \operatorname{div}\mathbf{S}^h\right]d\Omega \tag{7}
$$

in which the stability parameters $\alpha(\mathrm{Re}_K)$ and $\delta(\mathrm{Re}_K)$ are the ones proposed in Franca and Frey (1992), $\varepsilon << 1$ and β is set according to the suggestion of Behr *et al.* (1993).

Substituting the shape functions on the GLS formulation given by the Eqs. (5)-(7), a semi-discrete equation given by $\mathbf{R}(\mathbf{U})=0$ is obtained, in which $\mathbf{R}(\mathbf{U})$ is the residual of Eqs. (5)-(7) and $\mathbf{U}$ is the vector of the degrees of freedom of the primal variables $\boldsymbol{\tau}$, $\mathbf{u}$ and p. The solution of this semi-discrete system was implemented by employing a quasi-Newton method (Dahlquist and Bjorck, 1969), with the Jacobian matrix $\mathbf{J}(\mathbf{U})$ being updated at each iteration. The system of equations $\mathbf{J}(\mathbf{U}^k)\mathbf{a}^{k+1} = \mathbf{R}(\mathbf{U}^k)$ is solved to calculate the incremental vector $\mathbf{a}^{k+1}$, then the degree of freedom vector $\mathbf{U}^{k+1} = \mathbf{U}^k + \mathbf{a}^{k+1}$ is updated, until a convergence criterion, namely the norm of $\mathbf{R}(\mathbf{U}^k)$ smaller than a given tolerance, is achieved.

The above-stated problem is solved, first for inertialess flows. In this case, the results are obtained by employing a continuation strategy on Deborah number. In the sequence, inertia variation is achieved by using a continuation strategy on Reynolds number.

4. NUMERICAL RESULTS

In this section, the multi-field GLS approximation for the problem described by Eq. (4) – presented in equations Eqs. (5)-(7) – was employed for simulating an Oldroyd-B fluid flowing through a slot, depicted in Fig. 1. The numerical strategy has been described in the previous item. All results have been obtained by employing a finite element code under development at Laboratory of Computational and Applied Fluid Mechanics (LAMAC-UFRGS).

No-slip and impermeability boundary conditions are imposed at all the solid boundaries, namely at the upper and lower walls and at the slot boundaries. At boundaries assumed far away enough from the hole, so that the flow across them is not affected by its presence, fully developed Poiseuille profiles are considered, allowing determining velocity and extra-stress profiles at both sections.

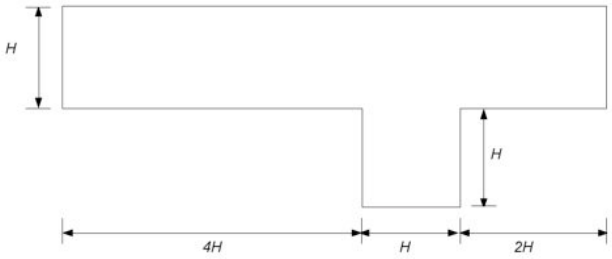

Figure 1. Problem statement: flow over a slot.

The viscoelastic flow governing dimensionless groups are Deborah and Reynolds numbers, defined, respectively, as

$$\mathrm{De} = \frac{\lambda \bar{u}}{H} \qquad \mathrm{Re} = \frac{\rho \bar{u} H}{\eta} \tag{8}$$

where $\bar{u}$ represents the average velocity at the channel entrance section and H is the channel height.

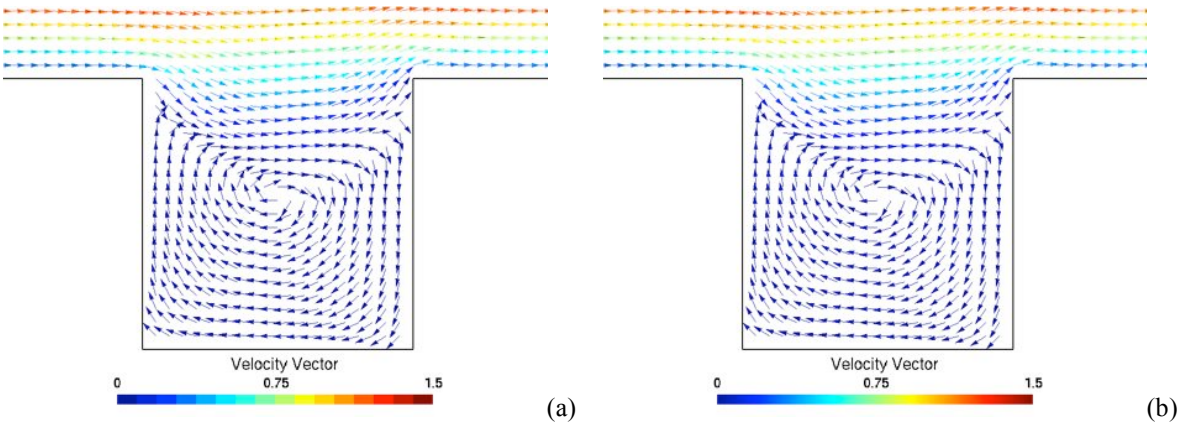

Figure 2. Velocity for Re=0: (a) De=0; (b) De=0.26.

Figures 2, 3 and 4 show the influence of viscoelasticity on an Oldroyd-B fluid inertialess flow through the slot depicted in Fig. 1. The velocity vectors depicted in Fig. 2 for De=0 and De=0.26 show that viscoelasticity variation has no influence on the velocity field, as observed by Huilgol and Phan-Tien (1997) – who have analytically determined the streamlines for a creeping flow across a slot.

Observing Fig. 3, it may be noted that the symmetry is progressively broken, due to the increasing elastic effects; i. e. the stress distribution becomes less symmetric as Deborah number increases. It is important to emphasize the increase in the maximum values of stress at the corners of the slot with Deborah number increase, for De=0, τ_{max}=4.05; for De=0.1, τ_{max}=7.29; for De=0.2, τ_{max}=11.3 and for De=0.26, τ_{max}=14.2, as may be observed in figure 4. In order to better visualize the results, the larger values have not been accounted for when the stresses were depicted in Fig. 3. Fig. 4 shows elevation plots for extra-stress considering the whole range of stresses. The larger values at the slot corners can be clearly visualized, mainly downstream the slot. Actually, Fig. 4 shows that the higher the viscoelasticity, the less symmetric are the extra stresses.

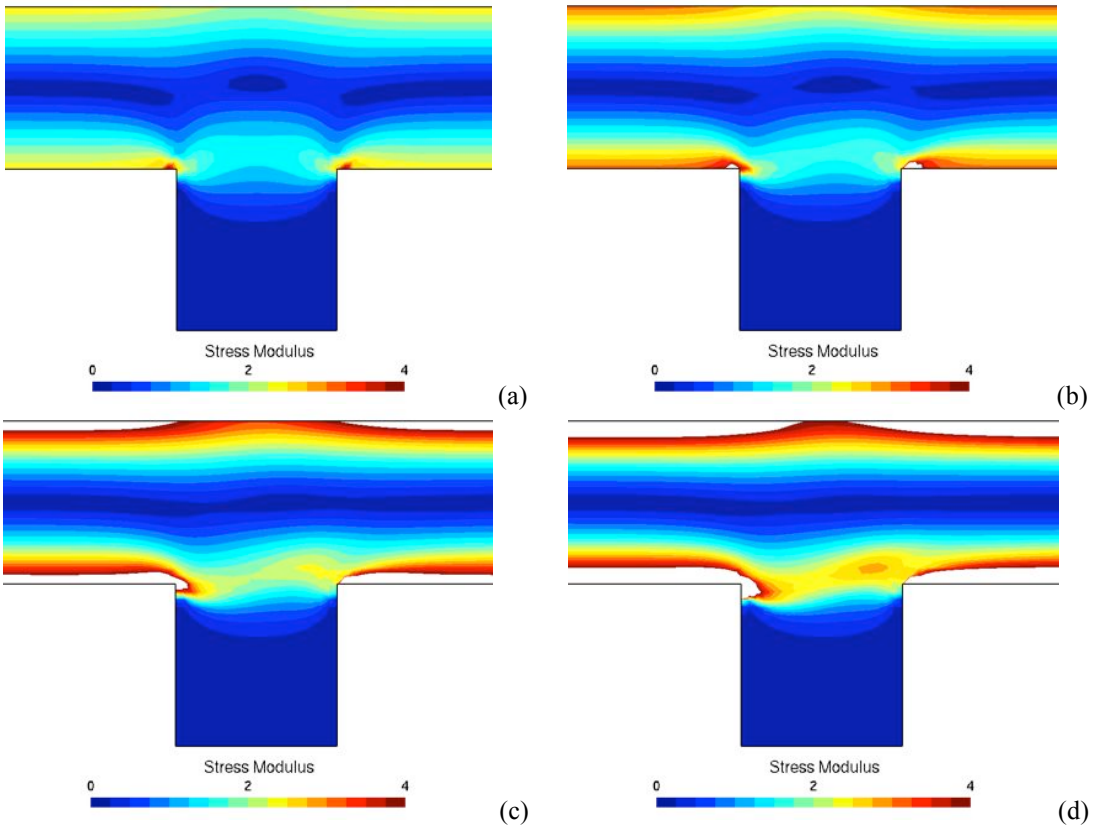

Figure 3. Extra-stress for Re=0: (a) De=0; (b) De=0.1; (c) De=0.2; (d) De=0.26.

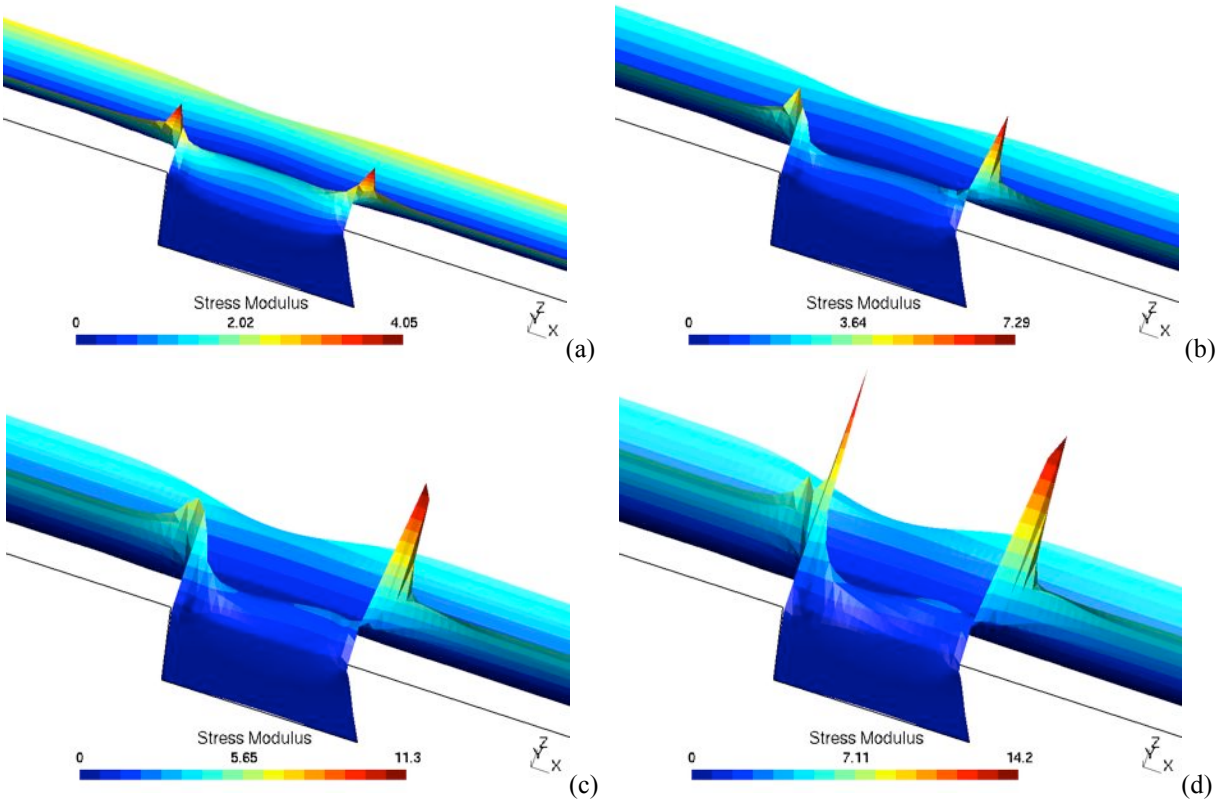

Figure 4. Extra-stress elevation plot for Re=0: (a) De=0; (b) De=0.1; (c) De=0.2; (d) De=0.26.

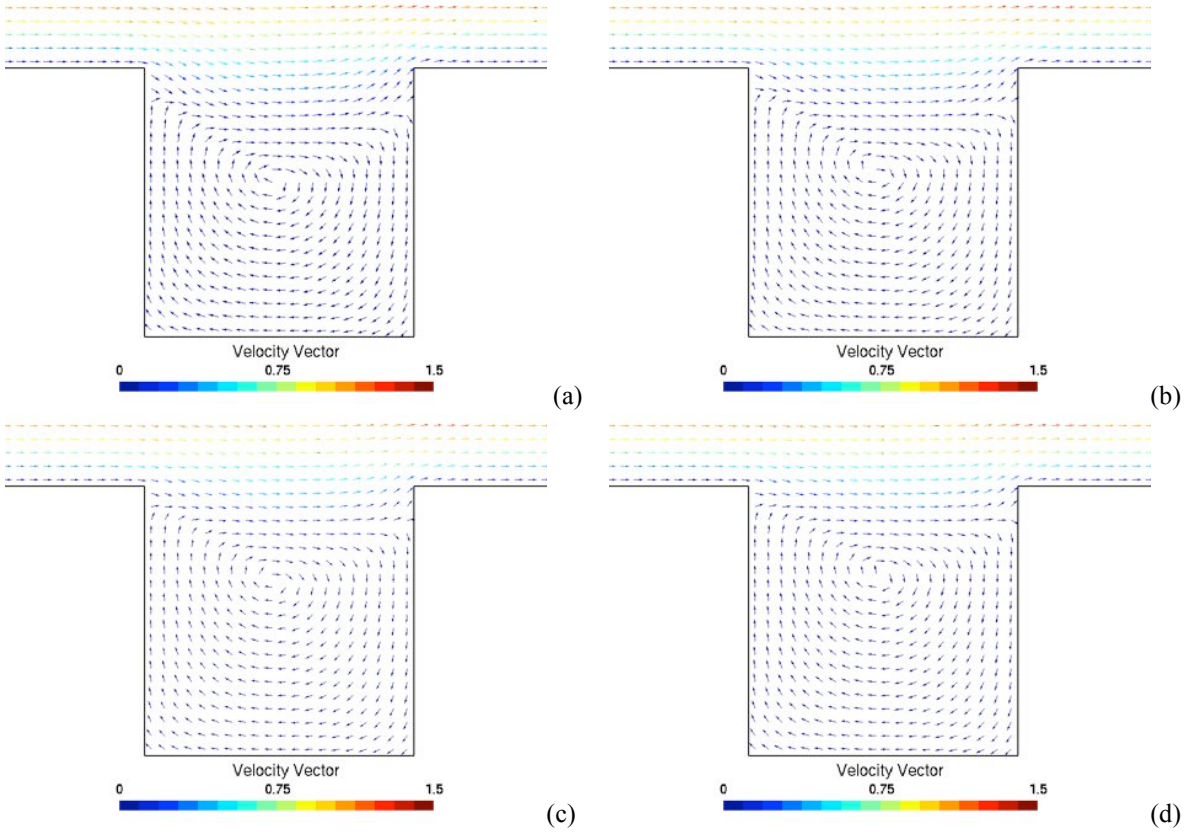

Figure 5. Velocity for De=0.26: (a) Re=5; (b) Re=10; (c) Re=15; (d) Re=20.

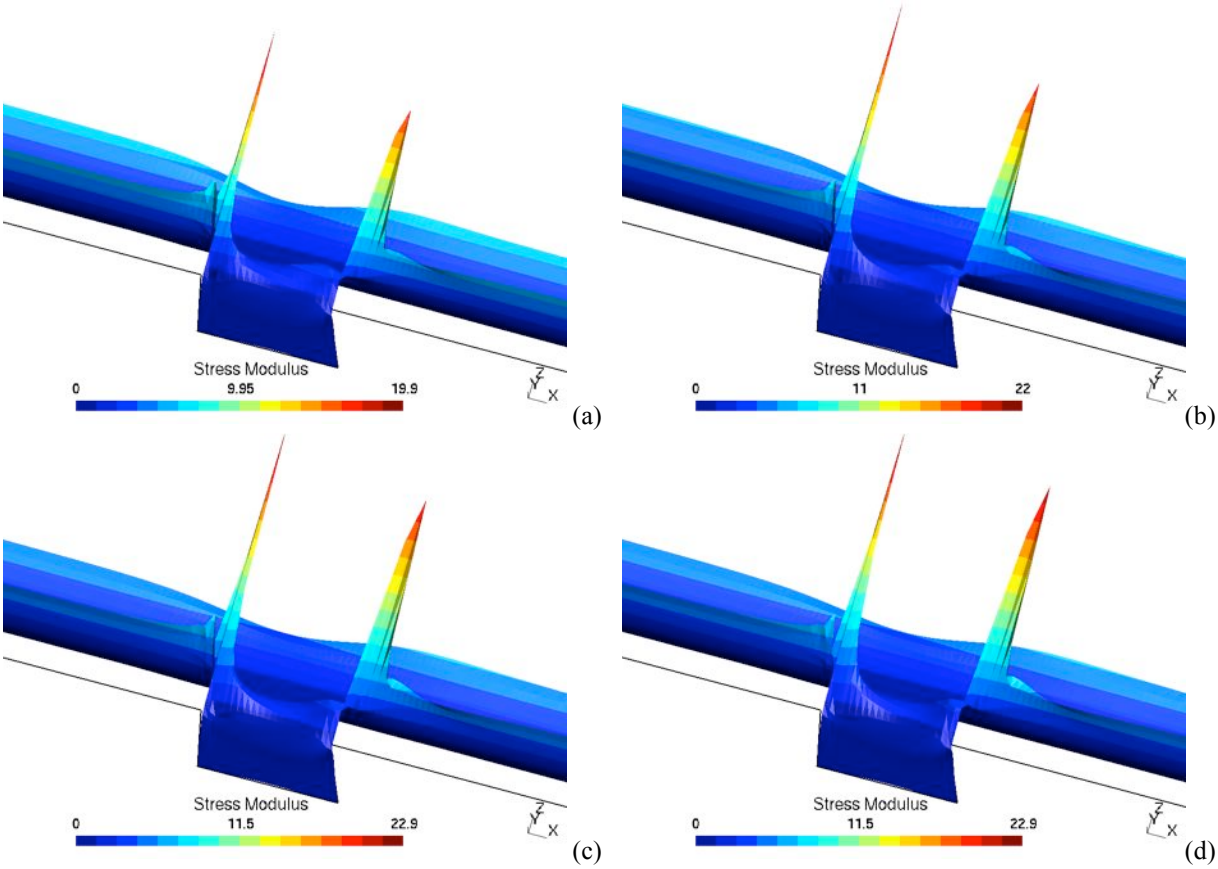

Figure 6. Extra-stress elevation plot for De=0.26: (a) Re=5; (b) Re=10; (c) Re=15; (d) Re=20.

Inertia effect on the velocity may be observed by comparing figures 2b (De=0.26; Re=0), 5a (De=0.26; Re=5), 5b (De=0.26; Re=10), 5c (De=0.26; Re=15) and 5d (De=0.26; Re=20). Reynolds number variation is not sufficient to provoke significant variation in the velocity field. Actually, a very small influence of inertia may be observed, with the vortex eye moving slightly upwards as Reynolds number increases and remaining at the position x^*=0 (the slot centerline).

Considering a viscoelastic flow (De=0.26), the inertia effect on extra-stress may be observed varying Reynolds number from 0 (as depicted the elevation plot shown in Fig. 4d) up to 20, in which Fig. 6 show extra-stress elevation plots for (a): Re=5; (b): Re=10; (c): Re=15 and (d): Re=20. It may be noted that the inertia increase causes a discrete enhancement in the maximum stress values at the upper wall neighborhood and both upstream and downstream the slot. Inertia increase also enhances stress concentration at the slot corners.

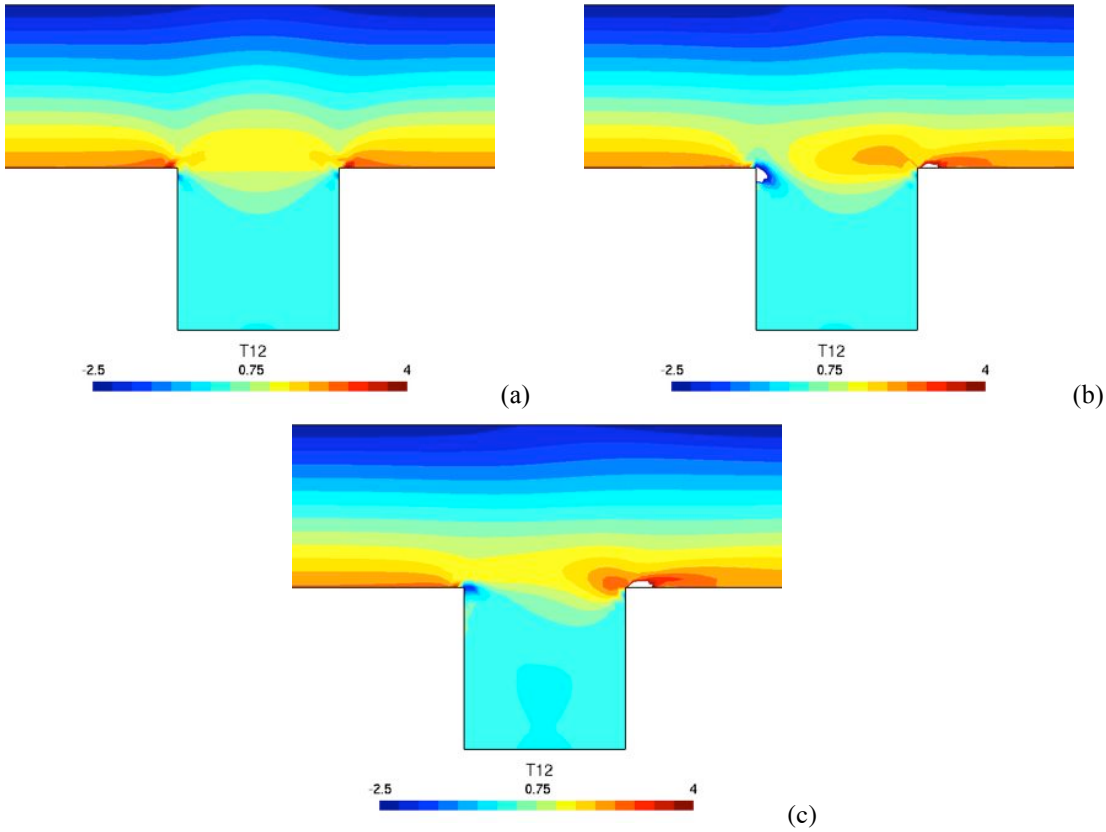

Figure 7. Shear stress for: (a) De=0 and Re=0; (b) De=0.26 and Re=0; (c) De=0.26 and Re=20.

Figures 7a and 7b show the viscoelasticity effect on shear stresses. Besides provoking an increasing asymmetry of the flow with the Deborah number increase, the shear stresses values also increase. Comparing Figures 7b and 7c, the inertia effect on a viscoelastic flow may be observed. The symmetry is affected by Reynolds number increase, which also causes a global decrease on the stresses and increases the stress concentration downstream the slot corner.

In order to validate the results, Figure 8 compares streamlines obtained in this work with the experimental results presented by Cochrane et al. (1981) for a convenient elastic test liquid – a dilute solution of polyacrylamide in a mixture of water and maltose syrup. The authors have carefully controlled the polymer concentration and the ratio of water to syrup, to minimize the dependency of the viscosity on the shear rate. In both figures the asymmetry both in the recirculating vortex and in the streamlines at the neighborhood of the slot may be clearly observed.

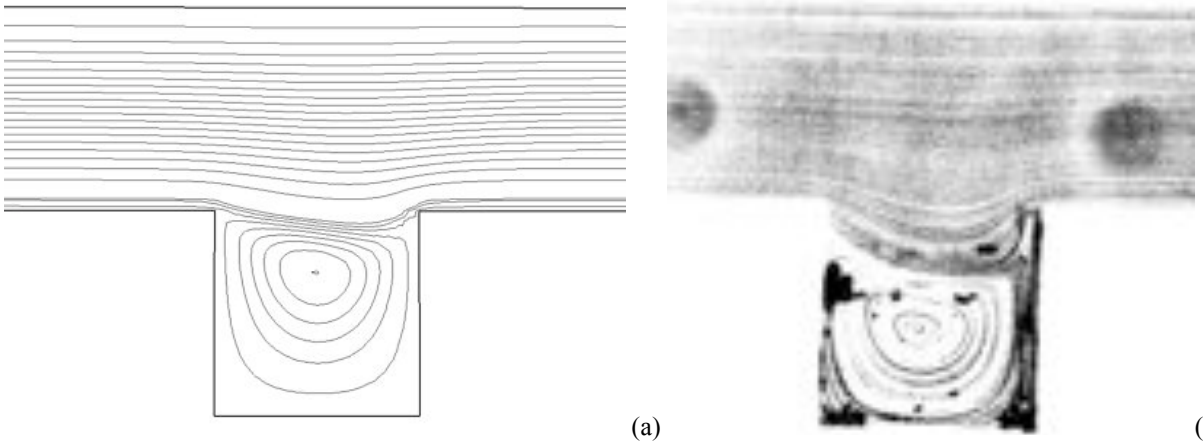

(a) (b)

Figure 8. Streamlines for De=0.2 and Re=10: (a) present work; (b) Cochrane et al. (1981).

5. FINAL REMARKS

A multi-field Galerkin least-squares finite element methodology, using as primal variables extra-stress, velocity and pressure, has been employed to approximate steady flows of an Oldroyd-B fluid though a slot. This stabilized formulation, characterized by a simple computational implementation, has adequately approximated viscoelastic flows and inertia flows, without satisfying neither the classical Babuška-Brezzi compatibility condition nor the compatibility between velocity and extra-stress subspaces. First, inertialess flows were considered, ranging Deborah number from 0 to 0.26. In the sequence, inertia was accounted for by ranging Reynolds number from 0 to 20. When De=0 and Re=0, neither elastic nor inertia effects are present, so extra-stress and velocity profiles are symmetrical. The symmetry is broken and the more viscoelastic the material, the higher the asymmetry. Inertia effects in viscoelastic flows increases the stress concentration at the slot corners, especially downstream as Reynolds number increases.

Furthermore, it must be emphasized that, thanks to the GLS methodology, the current simulations could be performed using an equal-order combination of finite element interpolations – more specifically, the bilinear ones – for all primal variables of the flow, namely extra-stress, pressure and velocity. In a straight comparison with the Galerkin method, such a combination, very attractive from the computation point-of-view, would simply not work. Another advantage over Galerkin, it is the ingenious scheme present in the GLS method to add selectively artificial diffusivity to advective- and diffusive-dominated flow regions, that allows achieving stable approximations even in high advective flows – a very attractive feature as elastic and inertia effects play a relevant role.

5. ACKNOWLEDGEMENTS

The authors S. Frey and M.L. Martins-Costa acknowledge Brazilian agencies CNPq and FAPERJ, for financial support.

6. REFERENCES

Alves, M. A., Oliveira, P. J. and Pinho, F. T., 2003, “Benchmark solutions for the flow of Oldroyd-B and PTT fluids in planar contractions”, J, Non-Newtonian Fluid Mech., Vol. 110, pp. 45-75.

Alves, M. A., Oliveira, P. J. and Pinho, F. T., 2004, “On the effect of contraction ratio in viscoelastic flow through abrupt contractions”, J, Non-Newtonian Fluid Mech., Vol. 122, 117-130.

Baaijens, F. P. T., 1998, “Mixed finite element methods for viscoelastic flow analysis: a review”, J. Non-Newtonian Fluid Mech., Vol. 79, pp. 361-385.

Babuška, I., 1971, “Error bounds for finite element methods”, Numerical Mathematics, Vol. 16, pp. 322-333.

Behr, M. A., Arora, D., Coronado-Matitti, O. and Pasquali, M., 2004, “Stabilized finite element methods of GLS type for Oldroyd-B viscoelastic fluids ”, Proceedings of ECCOMAS, pp. 1-15.

Behr, M. A. Franca, L. P. and Tezduyar, T. E., 1993, “Stabilized finite element methods for the velocity-pressure-stress formulation of incompressible flows”, Computer Methods Appl. Mech. Engng., Vol. 104, pp. 31-48.

Bird, R. B. Armstrong, R. C. and Hassager, O., 1987, “Dynamics of Polymeric Liquids”, Vol. 1: Fluid Mechanics”, 2nd ed., John Wiley & Sons, U.S.A.

Brezzi, F. 1974, "On the existence, uniqueness and approximation of saddle point problems arising from Lagrangian multipliers". RAIRO, Vol. 8-R2, pp. 129-151.

Brooks, A. N. and Hughes, T. J. R., 1982, "Streamline upwind/Petrov-Galerkin formulations for convection dominated flows with particular emphasis on the incompressible Navier-Stokes equation", Computer Methods Appl. Mech. Engrg., Vol. 32, pp. 199-259.

Ciarlet, P. G., 1978, "The Finite Element Method for Elliptic Problems", North-Holland, Amsterdam.

Cochrane, T., Walters, K. and Webster, M. F., 1981, "On Newtonian and non-Newtonian flow in complex geometries" Phil. Trans. R. Soc. London, Vol. 301, pp. 163-181.

Dahlquist, G. and Bjorck, A., 1969, "Numerical Methods", Prentice Hall, Englewood Cliffs, NJ, USA.

Franca, L. P., Frey, S. and Hughes, T. J. R., 1992, "Stabilized finite element methods: I. Application to the advective-diffusive model", Computer Methods Appl. Mech. Engrg. Vol. 95, pp. 253-276.

Franca, L. P. and Frey, S., 1992, "Stabilized finite element methods: II. The incompressible Navier-Stokes equations", Comput. Methods Appl. Mech. Engrg., Vol. 99, pp. 209-233.

Hughes, T. J. R., França, L. P. and Balestra, M., 1986, "A new finite element formulation for computational fluid dynamics: V. Circunventing the Babuska-Brezzi condition: A stable Petrov-Galerkin formulation of the Stokes problem accommodating equal-order interpolations", Computer Methods Appl. Mech. Engrg., Vol. 59, pp. 85-99.

Huilgol, R. R. and N Phan-Thien, N., 1997, "Fluid Mechanics of Viscoelasticiy" Elsevier Science, Netherlands.

Johnson, C. 1987, "Numerical Solution of Partial Differential Equations by the Finite Element Method", Cambridge University Press, Cambridge.

Oldroyd, J. G., 1958, "Non-Newtonian effects in steady motion of some idealized elastico-viscous liquids" Proc. R. Soc. Lond. Vol. 245, pp. 278-297.

Patankar, S.V., 1980, "Numerical Heat Transfer and Fluid Flow", Hemisphere Publishing Company, New York.

Sugeng, F. Phan-Thien, N. and Tanner, R. I., 1988, "A boundary-element investigation of the pressure-hole effect", J. Rheol., Vol. 32, pp. 215-223.

Tanner, R. I., 2000, "Engineering Rheology", 2nd ed., Oxford Press, Oxford.

Zinani, F. and Frey, S., 2008, "Galerkin least-squares multi-field approximations for flows of inelastic non-Newtonian fluids", J. Fluids Engineering, Vol. 130, pp. 815007.1-81507.14.

7. RESPONSIBILITY NOTICE

The authors are the only responsible for the printed material included in this paper.